Modelling of an Arbitrarily-Oriented Mobile Telephone Handset in the Finite-Difference Time-Domain Field Computation Method

P.S. Excell, P. Olley[1] and N.N. Jackson[2]

Department of Electronic and Electrical Engineering, University of Bradford, U.K.

([1]Now with Department of Mechanical Engineering, University of Bradford. [2]Now with School of Electrical Engineering & Science, Cranfield University, Royal Military College of Science, Shrivenham, UK)

ABSTRACT

The implementation of a generic mobile telephone handset model in the Finite Difference Time Domain (FDTD) method for computation of electromagnetic field distributions is described. The handset can be rotated about the principal FDTD axes to achieve any orientation. The 'thin wire' technique is used to model the antenna in a way that ensures that its correct electrical length is maintained despite the 'staircasing' effect of the FDTD grid. Computed predictions from the model agree with near-field measurements on a physical realisation of the handset, and accurate near and far fields are calculated for arbitrary orientations of the handset. It is concluded that this wire rotation technique has broad application to problems involving components that are required to move in relation to fixed structures.

1. INTRODUCTION

Computer modelling of the deposition of electromagnetic energy in the human head offers the opportunity to predict compliance of radiofrequency equipment with safety guidelines. Datasets representing heads, classified into regions with significantly different dielectric properties, have been modelled under irradiation by plane waves and dipoles [1,2] or mobile telephone handsets in simple orientations [3], and solid spheres have been irradiated by handsets [4] and plane waves [5,6]. Work specifically on the incorporation of handsets into FDTD software has been performed by Luebbers et al [7], Toftgard et al [4] and Jensen and Rahmat-Samii [8]. With dipole or handset irradiation, the antenna has almost invariably been oriented parallel to one of the principal FDTD axes, so that its wire (assumed straight) can be correctly represented in the FDTD mesh. However, the standard FDTD methods for representation of wires lead to errors if the antenna is not parallel to a principal axis as the resulting electrical length of the antenna is the sum of a sequence of orthogonal steps along FDTD cells (staircase approximation). In contrast, the physical length of the antenna is the linear distance between the initial and final cells: in general this will be significantly shorter than the FDTD discretised version.

A major consequence of this will be that the resonant frequency of the antenna will tend to be artificially depressed, and orientation-dependent, in the FDTD representation. The technique described below overcomes this limitation, allowing a handset to be located in a realistic orientation near a human head. This capability is vital for determination of the interaction of handsets with human tissue in realistic usage. In particular, realistic handset orientation is necessary to assess the Specific Absorption Rate (SAR) in the human head due to mobile telephones. (It may be noted that Jensen and Rahmat-Samii [8] allowed rotation of the handset relative to the head, but this was done by rotating the head rather than the handset: compensation for variation of the apparent length of resonant conductors was thus avoided).

A discussion of the accuracy that is estimated for the results presented below is given in Appendix 1.

2. THE THIN WIRE METHOD IN FDTD

The established method for representation of thin wires in an FDTD simulation is that suggested by Holland and Simpson [9]. In this technique each element of the antenna runs along an electric field component in a Yee cell [10] to form a continuous path from start to finish of the antenna. At each time step the driven point of the antenna is injected with a current, and the current on the tip of the antenna is maintained at zero.

The time-advance equation for an arbitrary element 'm' of the thin wire, located in cell (x,y,z)=(i,j,k) and pointing along the x-axis, is given by [9]:

$$I(m)^n = I(m)^{n-1} + \Delta t\left\{\frac{E_x(i,j,k)^{n-1/2}}{L} - \frac{Q(m+1)^{n-1/2} - Q(m)^{n-1/2}}{\varepsilon_0\mu_0\Delta x_{tw}}\right\} \quad (1)$$

where: $I(m)^n$ = current in wire element m
and $Q(m)^n$ = charge per unit length on wire element m

$E_x(i,j,k)^n$ = x component of electric field in cell (i,j,k) (each of the above are for time instant n)

Δt = FDTD time step

Δx_{tw} = 'corrected' length of thin-wire segment in x-direction

L = 'In-cell' inductance per unit length of the wire

The 'in-cell' inductance per unit length of the wire, L, ensures accurate treatment of the inductive fields close to the wire. It is given by [9]:

$$L = \frac{\mu_0}{2\pi}\left(\ln\left(\frac{R}{a}\right) - \frac{1}{2} + \frac{a^2}{2R^2}\right) \qquad (2)$$

where a is the wire radius, R is the effective radius of an FDTD cell and a<<R.

The 'corrected' segment length is found by multiplying the standard FDTD cell size in the x-direction by a correction factor to reduce the 'staircased' conductor length to equal the correct wire length. Elements parallel to the y or z-axes have analogous advance equations. The wire charges are similarly advanced, using:

$$Q(m)^{n+\frac{1}{2}} = Q(m)^{n-\frac{1}{2}} - \frac{\Delta t}{\Delta x_{tw}}\left(I(m)^n - I(m-1)^n\right) \qquad (3)$$

The electric fields are then updated by the currents, after their normal FDTD advance, by using:

$$E_x(i,j,k)^{n+\frac{1}{2}} = E_x(i,j,k)^{n-\frac{1}{2}} - \frac{\Delta t}{\varepsilon_0 \Delta y \Delta z} I(m)^n \qquad (4)$$

where Δy and Δz are the standard (not 'corrected') FDTD cell sizes in the y and z directions, Equation (4) being for the case where the wire segment is in the x-direction.

3. IMPLEMENTATION OF ROTATABLE HANDSET

To represent a generic mobile telephone handset, an antenna driven as a monopole and located on a dielectric-coated rectangular box was used. The cell at the base of the antenna was excited by a current of the form $I_0\sin(\omega t)$ and the charge in this cell was zeroed at each time step. The condition for the cell at the tip of the antenna was that the current be zeroed at each time step.

For a general-purpose model of the interaction between a handset and the human body it is normally most convenient to keep the body components fixed in the co-ordinate system and vary the orientation of the handset to simulate realistic usage. It is thus necessary to be able to generate a new, arbitrarily rotated, dataset from an existing handset geometry dataset. To define the handset structure it is usually most convenient to commence with the antenna oriented parallel to an axis of the FDTD mesh system (chosen to be the x-axis in the present work). It is convenient to define the origin to be at the base of the antenna: orientation is then defined as a pair of angles, first that for rotation about the z-axis, α, and then that for rotation about the y-axis, β (see Figure 1). This can readily be extended to include an additional rotation about the x-axis if required. The handset problem can then be separated into two distinct areas: rotating the antenna and rotating the handset body.

3.1 Rotatable Antenna

To overcome the problem of excessive electrical antenna length in a 'staircased' FDTD representation, a correction factor was introduced, in which the values of Δx_{tw} (and similarly Δy_{tw} and Δz_{tw}) used in Equations (1) and (3) were modified from the basic FDTD cell size by multiplication by a constant fractional factor f_w:

$$\Delta x_{tw} = f_w.\Delta x$$
$$\Delta y_{tw} = f_w.\Delta y$$
$$\Delta z_{tw} = f_w.\Delta z$$

$$\text{where } f_w = \frac{\text{Physical distance from antenna base to tip}}{\text{Staircased distance from base to tip}}$$

In this way the length of the antenna, as used in these equations, was independent of rotation angle.

The 'thin wire' technique requires the use of the above set of time-advance equations (in addition to the standard FDTD time-marching equations) for each cell through which the wire passes. The following algorithm generates the necessary parameters for use in Eqns (1), (3) and (4).

If the base of the antenna is defined as the origin (0,0,0), the end point, $(x_{end},y_{end},z_{end})$ is calculated thus:

$$x_{end} = R\cos(\alpha)\cos(\beta)$$
$$y_{end} = R\sin(\alpha)$$
$$z_{end} = -R\cos(\alpha)\sin(\beta)$$

where α is the angle rotated about the z-axis, β is the angle then rotated about the y-axis and R is the antenna length. The FDTD cell indices of the base and end of the antenna may then be ascertained.

It is next necessary to calculate the shortest continuous 'staircased' path of electric fields between the two ends, this path following the electric field components in the Cartesian grid of FDTD cells. This may be performed by noting the indices of each new cell traversed by a straight line from base to tip of the antenna. The following examples show how the components and positions of electric fields required to form such a thin wire may be deduced.

If two consecutive cells are denoted by (i,j,k) and (i+1,j,k), then the E_x component located in cell (i+1,j,k) is required to link the two cells. Similarly, the E_x component located in cell (i,j,k) is required to link the consecutive cells (i-1,j,k) and (i,j,k) (see Figure 2). In the cases where two indices change between consecutive cells, the corresponding two electric field components will be needed. For example, a step from cell (i,j,k) to cell (i+1,j+1,k) requires the E_x field component of cell (i+1,j,k) and then the E_y field component of cell (i+1,j+1,k) (see Figure 3). A list of lattice positions and components of the electric fields necessary to step from base to tip of the antenna may thus be deduced. These can then be used directly in Equations (1), (3) and (4) above.

It was found that the formulation of Equations (1) and (4) fails if the chosen direction of conventional positive current flow in the wire segment under consideration is antiparallel to the corresponding unit vector of the co-ordinate system. To cover such cases these equations had to be modified as follows:

$$I(m)^n = I(m)^{n-1} + \delta(m)\Delta t\left\{\frac{E_x(i,j,k)^{n-1/2}}{L} - \frac{Q(m+1)^{n-1/2} - Q(m)^{n-1/2}}{\varepsilon_0\mu_0\Delta x_{tw}}\right\} \quad (5)$$

$$E_x(i,j,k)^{n+\frac{1}{2}} = E_x(i,j,k)^{n-\frac{1}{2}} - \delta(m)\frac{\Delta t}{\varepsilon_0\Delta y\Delta z}\, I(m)^n \quad (6)$$

where $\delta(m) = +1$ if the defined direction of positive current flow in element 'm' is parallel to the unit x-vector, and $\delta(m) = -1$ if the positive current flow direction is defined to be antiparallel to the unit vector.

3.2 Rotatable Handset Body

As shown by Luebbers *et al* [7], the electrical properties of many practical handsets may be realistically represented by an antenna on a metal chassis surrounded by a dielectric (plastics) case. Consider first the metal chassis oriented with its principal axis parallel to the x-axis as in Figure 1: let the point at which the antenna and chassis meet be defined as position (0,0,0) and let an arbitrary point on the metal chassis be (x_m,y_m,z_m) with reference to this origin. As was the case for the antenna, this point can be rotated by α about the z-axis and then β about the y-axis to get the position after rotation $(x_{rot},y_{rot},z_{rot})$. This position is given by calculating the intermediate position (x_1,y_1,z_1) after rotation by α about the z-axis, then calculating the position after a further rotation by β about the y-axis, viz.:

$$x_1 = r_0\cos(\theta_0 + \alpha)$$
$$y_1 = r_0\sin(\theta_0 + \alpha)$$
$$z_1 = z_m$$

where $\theta_0 = \tan^{-1}(y_m/x_m)$
and $r_0 = (x_m^2 + y_m^2)^{1/2}$

Then:

$$x_{rot} = r_1\sin(\theta_1 + \beta)$$
$$y_{rot} = y_1$$
$$z_{rot} = r_1\cos(\theta_1 + \beta)$$

where $\theta_1 = \tan^{-1}(z_1/x_1)$
and $r_1 = (x_1^2 + z_1^2)^{1/2}$

Each point represents a location on the metal chassis after rotation. The lattice cell indicated by each such point is easily calculated and its position must be stored for later use during time stepping. At each time step, the tangential electric field components on the metal surface must be zeroed. In a staircased representation this is achieved by zeroing all three orthogonal components in any cell deemed to contain metal.

Similarly, the dielectric case of the handset may be rotated. In this case it is necessary only to set correct electrical properties for the indicated lattice cells. In general, any dielectric or perfectly conducting metal shape may be rotated in this manner.

4. RESULTS

Numerical tests were undertaken with an FDTD program based on THREDE [11], but using Fang-Mei superabsorbing boundary conditions as the interface to free space [12]. In addition, a near-to-far field transformation algorithm (see below) and the modifications described above were incorporated into the program. The computer was a Sun Sparcstation 10 with 96Mbyte main memory.

4.1 Near Fields

A battery-powered transmitter simulating the generic shape of typical commercial handsets was constructed. This radiated 1.8GHz CW from a $\lambda/4$ monopole located on the top surface of a rectangular case. The case was made of plastics material (with ε_r=2.0, as in [7]) with a conducting inner coating. This was placed in an anechoic chamber, and near-field measurements of the x-component of the electric field were made over the volume shown in Figure 4. An FDTD representation of a handset with the same dimensions was constructed and the same field component was calculated. Figure 5 shows the electric field intensity in a series of planes at regular intervals away from the handset. The measured results can be seen to compare very closely with results from FDTD analysis in the region close to the handset. The discrepancy appears to increase somewhat at larger distances (maximum error within 3dB), but the agreement can still be said to be good, given the difficulties of representing the exact structure of a simulated handset assembled from commercial components, and errors inherent in field strength measurements with a small dipole probe. The results can be said to demonstrate the validity of Luebbers' model of an antenna on a plastic coated metal chassis [7] in the near field.

Figure 6 shows the total electric field magnitude, as calculated by the FDTD method, in the arrangement described above. Also shown are the results calculated by rotating the FDTD handset model by 45° about the z-axis. The results for the rotated handset are seen to give excellent agreement with those for the axially-aligned handset.

The far field was also calculated for the axially aligned and rotated handsets using the near-to-far field transformation method described by Taflove & Umashankar [13]. Figure 7 shows the far-field radiation pattern in the x-y plane for both orientations: the results from the rotated handset have been rotated back by 45° to enable direct comparison to be made. The amplitudes are in good agreement, with a slight angular offset. Empirically, the angle of error has been found to be of the order of 1/N radians, where N is the number of cells in the FDTD antenna. This indicates that quantization is the cause of the angular error: use of finer FDTD meshes reduces it.

4.2 Output Power

The power radiated by the FDTD handset model was measured for a range of orientation angles. Although the radiation patterns were in excellent agreement for all orientation angles, it was found that the actual power radiated was dependent upon orientation. Let the angle β now be defined as the angle between the antenna and the x-axis in the x-z plane (see Figure 1). The FDTD handset model was set to a number of values of β between 0 and $\pi/2$ and the radiated power was computed in each case. The power calculation was performed by summing the outgoing component of the Poynting vector over a closed surface surrounding the handset. Figure 8 shows the power transmitted as a function of angle when the monopole was fed with 1A peak CW at 1.8GHz. The FDTD cells were cubes with side lengths of 2.5mm, corresponding to approximately $\lambda/33$ in free space.

The radiated power can be seen to vary by around 20% as the angle is varied. The power output is symmetrical about the $\pi/4$ orientation as would be expected in a cubic FDTD mesh. It was suspected that the variation might be due to quantization errors in the length of the antenna and the handset body. The antenna is required to be terminated by zeroing the current in its end segment. As different orientations imply differing values of Δx_{tw}, Δy_{tw} and Δz_{tw} the 'thin wire' antenna may be expected to be a source of error, since end segments of varying lengths would be partially excluded from the electrical length.

Fig. 9 shows the currents along the antenna for orientations between 0 and 45°. The results are symmetrical about 45° so results from 45 to 90° are not shown. The currents follow a similar pattern, but with discrepancies of up to 10%, which might account for the 20% variation in total power. To study this phenomenon further, the same problem was re-computed using a reduced cell size of 1.25mm ($\lambda/67$). Figures 10 and 11 show the power and current for a range of orientation angles at this resolution. The variation in power (Figure 10) is reduced to 6% maximum, and the variation in current (Figure 11) is nowhere higher than 7% along the lengths of the wires. The relatively large drop in power variation, compared with the result for $\lambda/33$ resolution, suggests that the handset body may be equally responsible for power variations. The finer cell size enables the representation of a rotated body to be electrically more exact. The marked improvement in correlation of both power outputs and currents, as resolution improves, indicates that the small discrepancies originate from quantization errors, not errors in the method. It is important to note that, when field patterns are normalised to 1 Watt output (as is normal in the Specific Absorption Rate (SAR) calculations, for which the rotatable handset model has

been developed), both near and far-field patterns are in excellent agreement at all orientation angles.

5. CONCLUSION

It has been shown that the 'thin wire' technique can be used as a basis for modelling an arbitrarily-oriented handset (or some other structure made of dielectrics and metal) in an FDTD lattice. Both near and far fields are in good agreement with the results for a handset in the 'conventional' orientation, i.e. with principal dimensions parallel to the Cartesian axes, and the near fields also agreed well with physical measurements. This technique has particular application to the calculation of the interaction between realistically-oriented portable handsets and the human body. The technique for rotating a solid object in an FDTD lattice has broad application to problems involving two or more physical entities that may be re-positioned in relation to each other (e.g. helicopter rotors and microwave oven interiors). One or more of the objects can be positioned, and repositioned, relative to others without significant restructuring of the program or input data.

REFERENCES

[1] P.J. Dimbylow and O.P. Gandhi, 'Finite-Difference Time-Domain Calculations of SAR in a Realistic Heterogeneous Model of a Head for Plane Wave Exposure from 600MHz to 3GHz', Phys. Med. Biol., Vol. 36, No. 8, pp 1075-1089, 1991

[2] P.J. Dimbylow, 'FDTD Calculations of the SAR for a dipole closely coupled to the head at 900MHz and 1.9GHz', Phys. Med. Biol., Vol. 38, pp 361-368, 1992

[3] P.J. Dimbylow and S.M. Mann, 'SAR calculations in an anatomically realistic model of the head for mobile communication transceivers at 900MHz and 1.8GHz', Phys. Med. Biol., Vol. 39, pp 1537-1553, 1994

[4] J. Toftgard, S.N. Hornsleth and J.B. Andersen, 'Effects on Portable Antennas by the Presence of a Person', IEEE Trans. Antennas & Propagation, Vol.41, No. 6, pp 739-746, 1993

[5] H.N. Kritikos and H.P. Schwan, 'Hot Spots Generated in Conducting Spheres by Electromagnetic Waves and Biological Implications', IEEE Trans. Biomed. Eng., Vol. BME-19, No. 1, pp 53-58, 1972

[6] A.R. Shapiro, R.F. Lutomirski and H.T. Yura, 'Induced Fields and Heating Within a Cranial Structure Irradiated by an Electromagnetic Plane Wave', IEEE Trans. Microwave Theory & Tech., Vol. MTT-19, No. 2, pp 187-196, 1971

[7] R. Luebbers, L. Chen, T. Uno and S. Adachi, 'FDTD Calculation of Radiation Patterns, Impedance and Gain for a Monopole Antenna on a Conducting Box', IEEE Trans. Antennas & Propagation, Vol. 40, No. 12, pp 1577-1583, 1992

[8] M.A. Jensen and Y. Rahmat-Samii, 'EM Interaction of Handset Antennas and a Human in Personal Communications', Proc. IEEE, Vol. 83, No. 1, pp 7-17, 1995

[9] R. Holland and L. Simpson, 'Finite Difference Analysis of EMP Coupling to Thin Struts and Wires', IEEE Trans. Electromag. Compat., Vol. EMC-23, No. 2, pp 88-97, 1981

[10] K.S. Yee, 'Numerical Solution of Initial Boundary Value Problems involving Maxwell's Equations in Isotropic Media', IEEE Trans. Antennas & Propagation, Vol. AP-14, pp 302-307, 1966

[11] R. Holland, 'THREDE: A Free-Field EMP Coupling and Scattering Code', IEEE Trans. Nucl. Sci., Vol. NS-24, No. 6, pp 2416-2421, 1977

[12] K. K. Mei and J. Fang, 'Superabsorption - A Method to Improve Absorbing Boundary Conditions', IEEE Trans. Antennas & Propagation, Vol. 40, pp 1001-1010, 1992

[13] A. Taflove and K. Umashankar, 'Radar Cross Section of General Three-Dimensional Scatterers', IEEE Trans. Electromag. Compat., Vol. EMC-25, No.4, pp 433-440, 1983

Acknowledgement

This work was supported by the UK SERC/DTI 'LINK' Personal Communications Programme and a consortium of nine companies. Purchase of THREDE source code from EMA Inc. was funded by a grant from the University of Bradford Research Committee.

APPENDIX 1
Quantitative Accuracy Statements

1. An estimate of the accuracy of the results presented here can be made from examination of the comparisons

presented in Figs 5, 6, 7, 9 and 11, and from a comparison of Figs 8 and 10.

In Fig. 5, it is seen that the shapes of the computed near-field distributions agree well with the measured results (normalised to equality at identical central points) and the maximum magnitude discrepancy is within 3dB. Experience suggests that this discrepancy is partly caused by the limitations of the quantised FDTD representation of the handset structure and partly by measurement uncertainty. Fig. 6 indicates that computed near field results are stable to within 1dB under rotational transformation with respect to the FDTD mesh.

Fig. 7 indicates stability in the peak far field gain of better than 0.5dB under rotational transformation. Errors of the order of 10dB may occur in deep nulls, but this is a common problem which could be reduced by using a smaller cell size.

Comparison of Figs 8 and 10 shows that the cell size of $\lambda/33$ used to produce the above results also leads to variations of about ± 0.5dB in the radiated power under rotational transformation, but that halving the cell size reduces this to ± 0.12dB.

Fig. 9 indicates maximum variations of about ± 0.2dB in the antenna current distribution under rotational transformation with a cell size of $\lambda/33$, reducing to ± 0.13dB with $\lambda/67$ cells (Fig.11).

2. These estimates are based on measurement (Fig. 5), co-ordinate transformation and variation of discretisation intervals.

3. The kinds of problems for which the above error/accuracy statements can be made for this program include the modelling of current distributions, near and far fields for arbitrary structures of conductor and dielectric, with maximum dimensions up to about a wavelength.

4. Nominal sampling densities required to achieve these estimated accuracies are $\lambda/33$ in most cases ($\lambda/67$ where indicated).

5. The operation count needed to exercise the model reported here is estimated nominally to be of the order of $10^{12}f^{-1}$, where f is in Hz.

6. The variable storage needed to exercise this model is estimated nominally to be 1Mword for $\lambda/33$ sampling density (8Mwords for $\lambda/67$). This is based on the modelling of a simulated handset at 1.8GHz, where $\lambda/33$ = 5mm. The model, with the same absolute dimensions and sampling interval, could be used down to about 1GHz, below which the free-space margin between conductors and the absorbing boundary would have to be increased; it should also remain stable up to about 4GHz (based on sampling interval considerations), although substantial errors would begin to appear in some parameters.

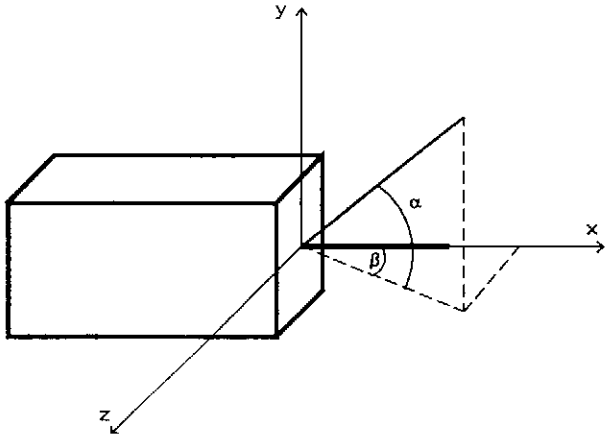

Fig.1 The simulated generic handset, associated co-ordinate system and rotation angles.

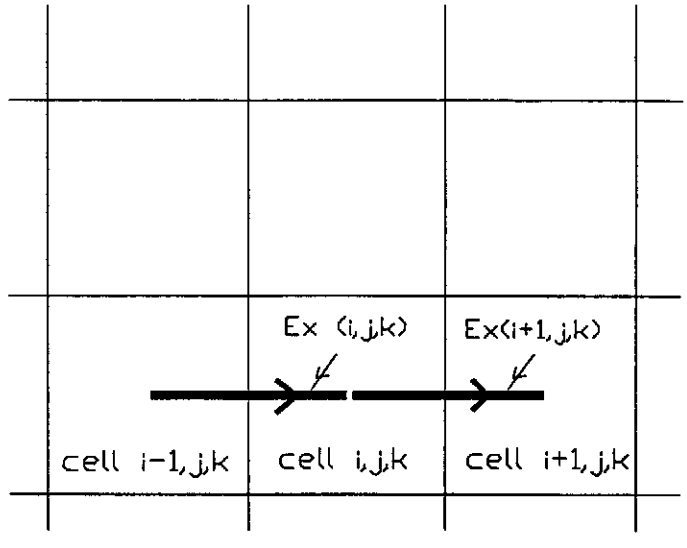

Fig.2 Rectilinear linkage of electric field components between adjacent FDTD cells: a continuous sequence of such links is needed to represent a thin wire.

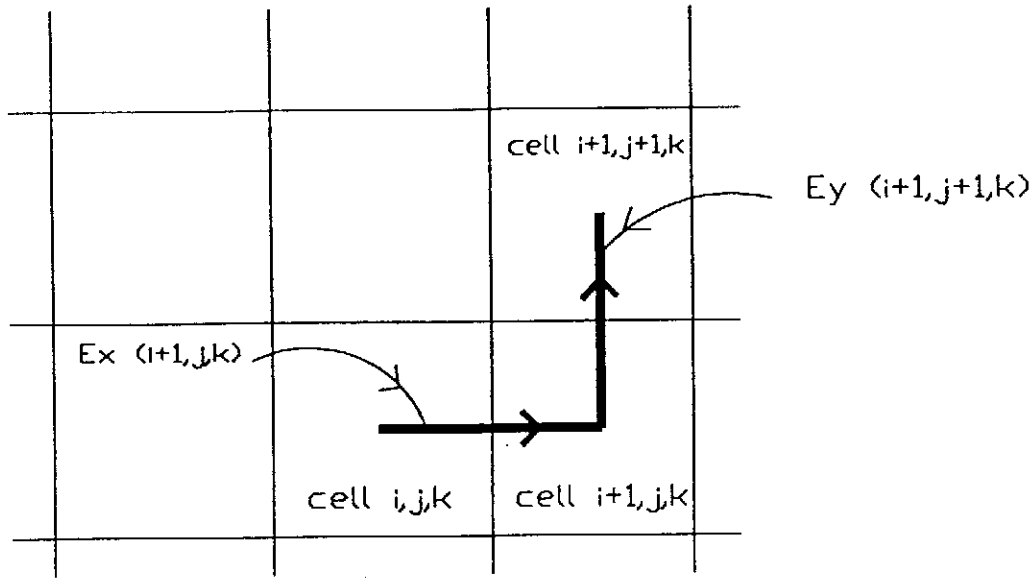

Fig.3 Angled linkage of electric field components between non-rectilinear sequences of FDTD cells.

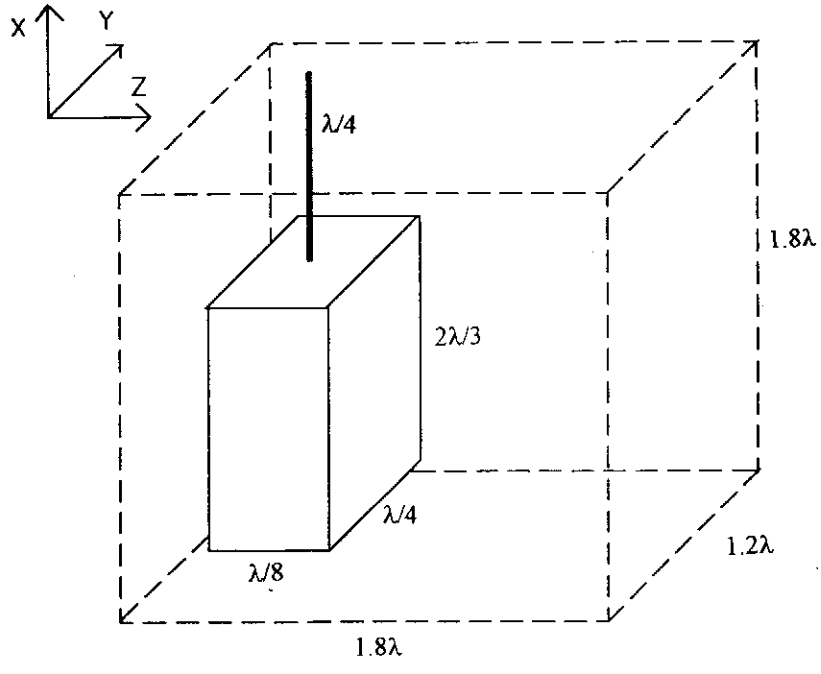

Fig.4 Dimensions of handset and volume over which fields were computed and measured. Dimensions are given in free-space wavelengths at 1.8GHz.

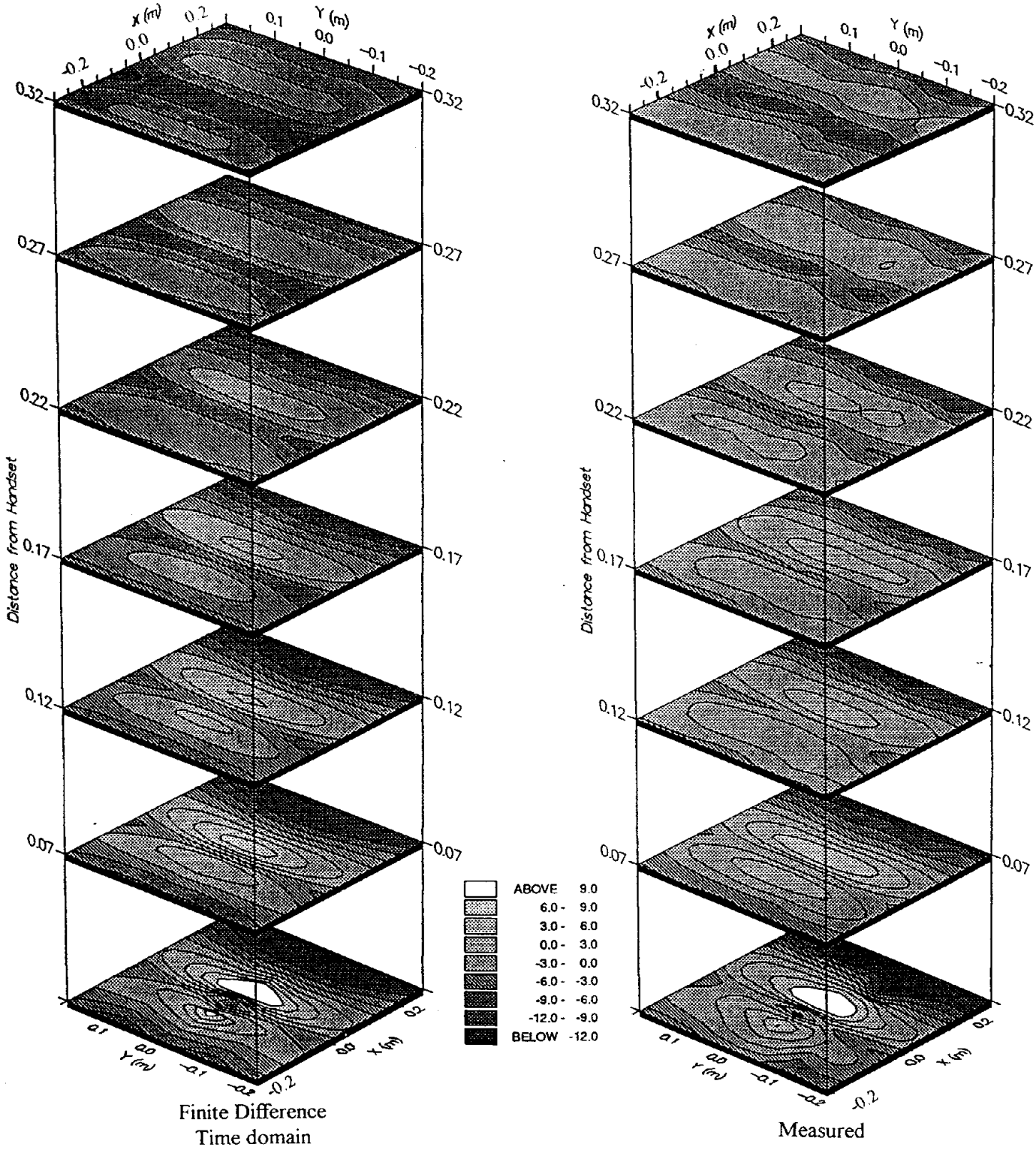

Fig.5 Magnitude in dB of the x-component of the electric field over several planes normal to the z-axis: (a) as computed by FDTD; (b) as measured. Both plots are normalised to their respective amplitudes at the centre of the plane 0.17m from the handset.

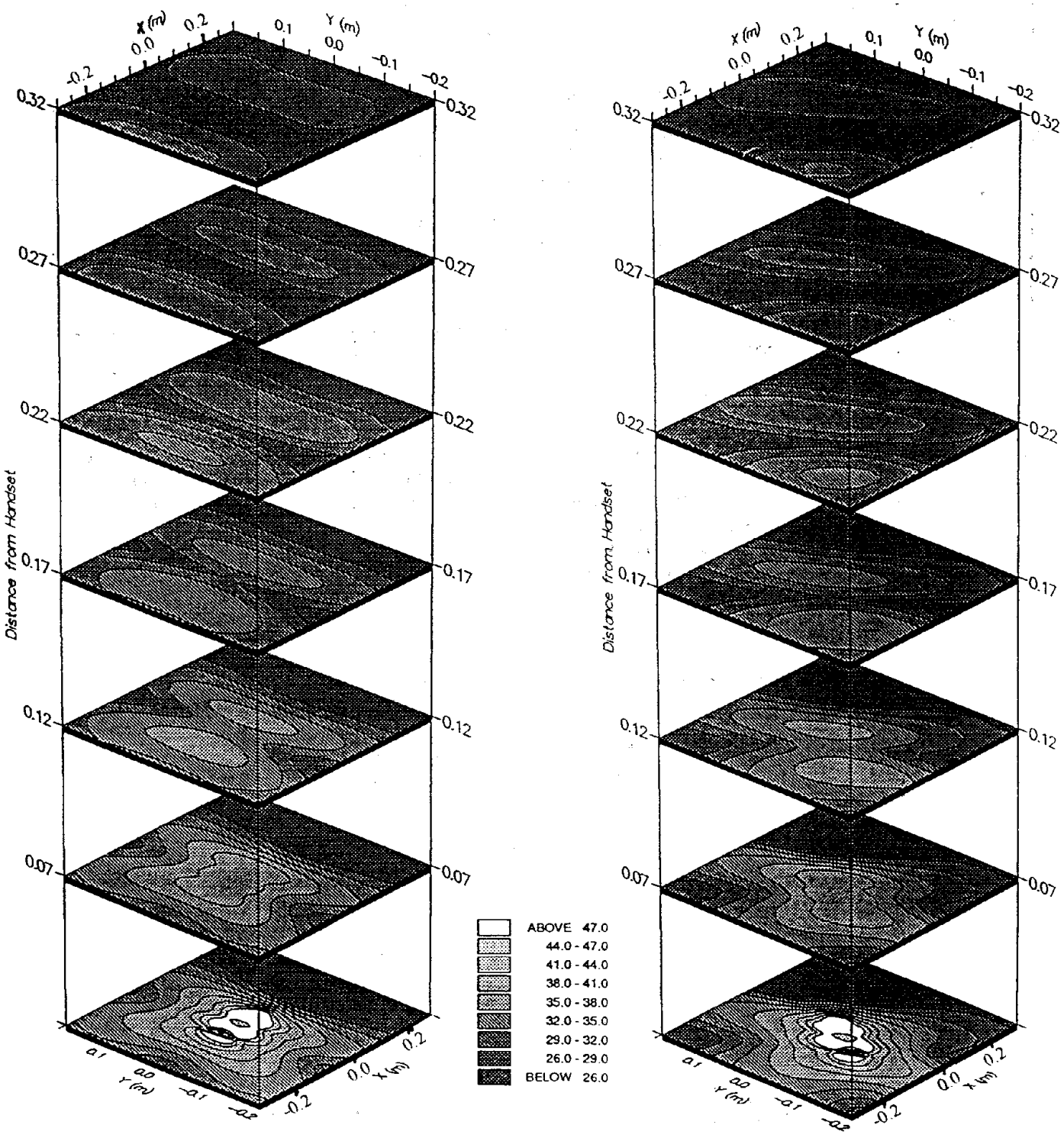

Fig.6 Magnitude (in un-normalised dB) of the total electric field (|E|) over several planes normal to the z-axis as computed by FDTD: (a) handset axially-aligned; (b) handset rotated 45° about z-axis.

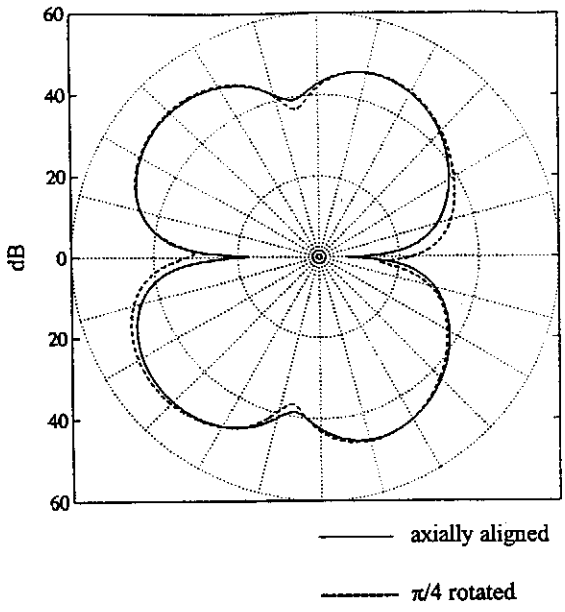

Fig.7 Far-field pattern in plane z=0, as computed by FDTD with handset axially oriented (solid curve) and rotated 45° about z-axis (the broken curve shows the result as rotated back by -45° to facilitate comparison). Scale is in dB relative to the same reference level, with a constant offset added to make all results positive.

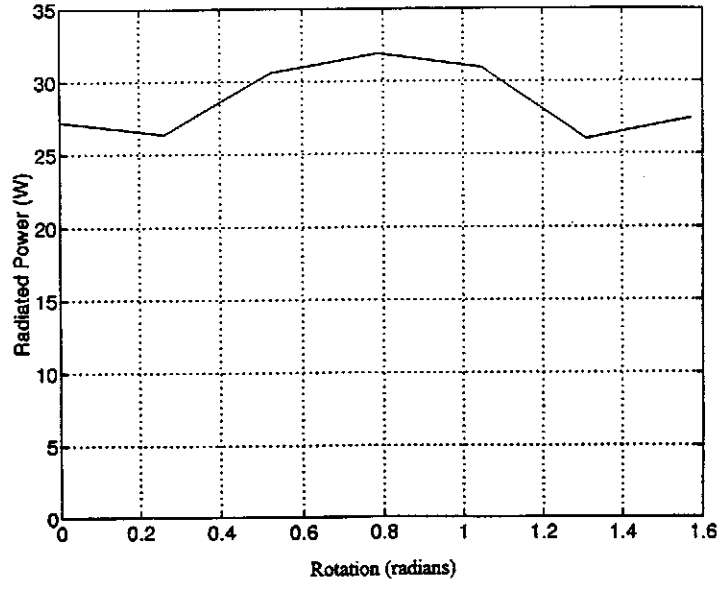

Fig.8 Total radiated power predicted by FDTD (mesh interval = λ/33), for constant antenna feedpoint current, as a function of handset rotation angle.

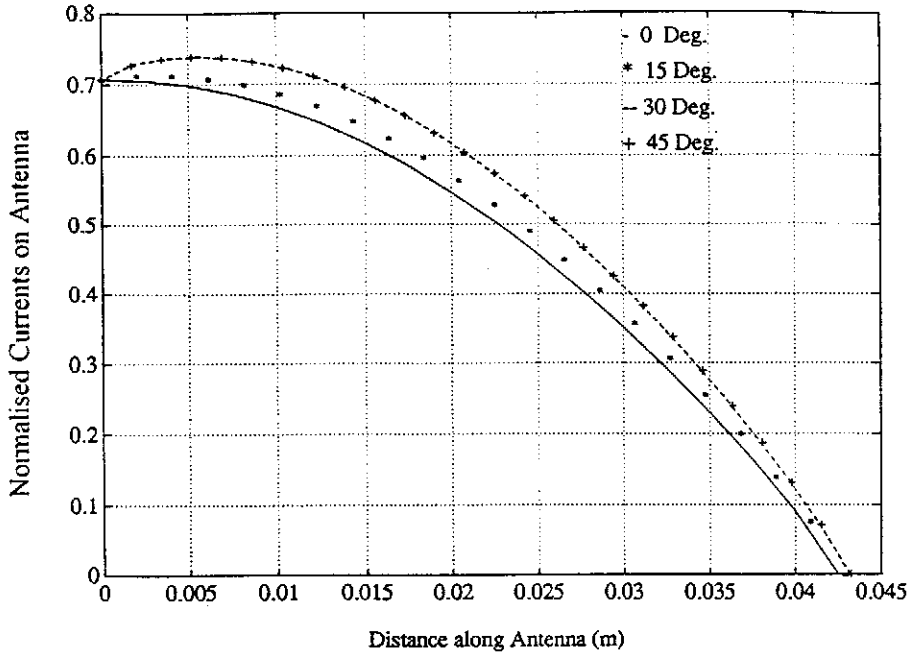

Fig.9 Variation of computed current distribution in the monopole with rotation of the handset, for FDTD mesh interval of λ/33. Normalised current is displayed as the ratio of local r.m.s. value to peak driving current at base of antenna.

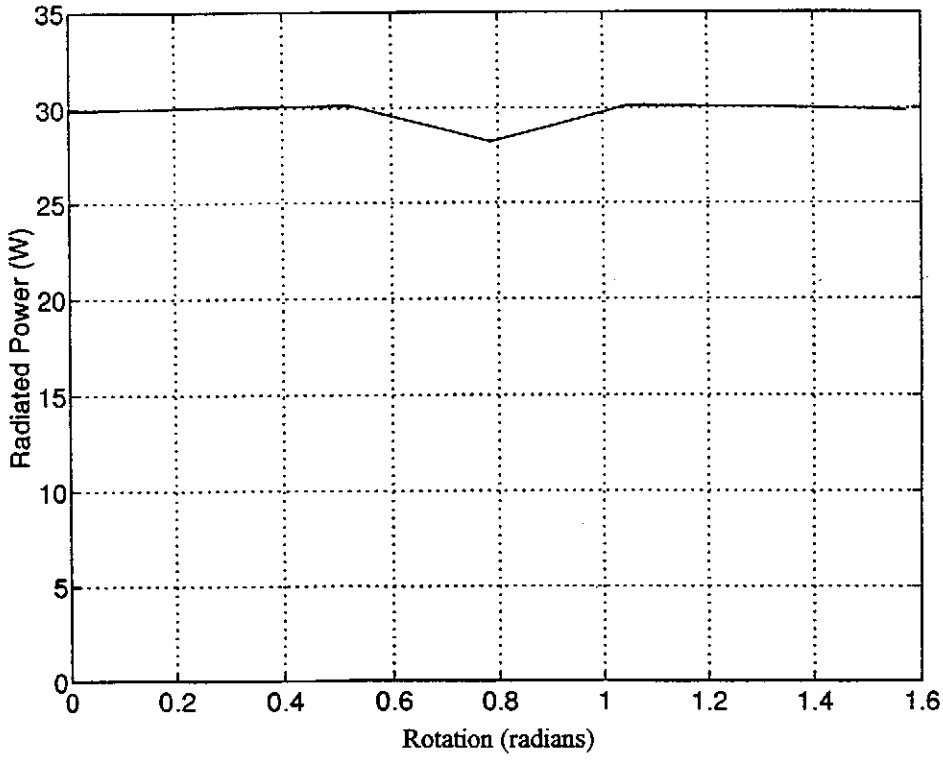

Fig.10 Total radiated power as a function of orientation angle, for FDTD mesh interval of $\lambda/67$.

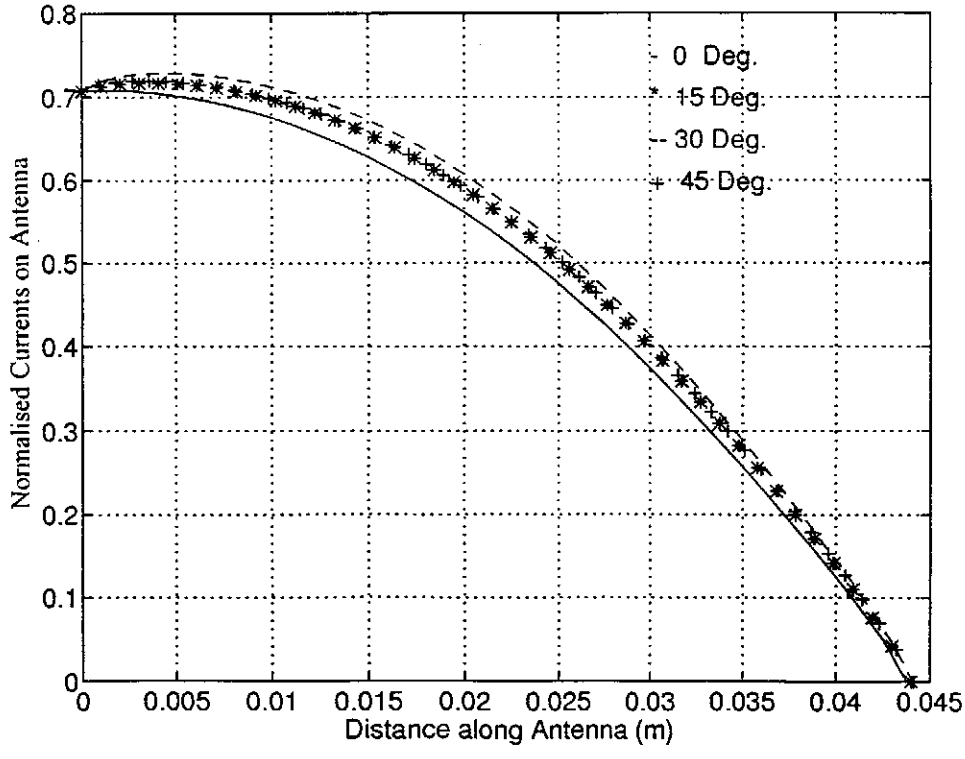

Fig.11 Variation of computed current distribution in the monopole with rotation of the handset, for FDTD mesh interval of $\lambda/67$ (Current normalised as in Fig. 9).